Self-Switching Vibrating Micromechanical Filter Bank

Sheng-Shian Li, Yu-Wei Lin, Zeying Ren, and Clark T.-C. Nguyen

Center for Wireless Integrated Micro Systems
Department of Electrical Engineering and Computer Science
University of Michigan, Ann Arbor, Michigan 48109-2122, USA

Abstract—**Bridged MEMS-based micromechanical filters have been demonstrated that use a self-switching property of their dc-biased capacitive transducers to achieve zero-loss on/off filter switching without the need for lossy series switches, and with settling times down to 1.5 μs. By dispensing with the need for series switches in the signal path, a small bank of 0.087% bandwidth, 9-MHz beam-based filters has achieved programmable channel/band selection with only 3 dB of insertion loss, comprised entirely of filter loss (i.e., no switch loss), with switching times 7x faster than the typical 10 μs of some of the fastest RF MEMS switches, and without the high actuation voltages (>90V) and reliability issues often associated with RF MEMS switches. Higher frequency 155-MHz disk resonators achieve even faster switching speeds, with settling times down to only 430 ns. Equipped with this self-switching property, capacitively transduced micromechanical resonators are attractive candidates for realization of the switchable filter banks targeted for future wireless transceivers.**

Keywords—**MEMS, micromechanical, capacitive transducer, filter bank, self-switching, switching speed, RF MEMS switch, resonator, channel selection.**

I. INTRODUCTION

With their tiny size, high on-chip integration density, and Q's in the thousands at GHz frequency, micromechanical resonators are poised to make possible new communication architectures that harness high Q elements in massive numbers to lower power consumption and enhance robustness against jamming interferers. To illustrate, Fig. 1 presents system block diagrams depicting (a) a direct conversion receiver [1][2] that attempts to minimize as much as possible the number of off-chip high Q frequency control components used, sacrificing power consumption and robustness against interferers in the process; and (b) a targeted receiver topology that takes advantage of MEMS technology and uses micromechanical circuits in abundance (with little or no size or cost penalty) to realize a front-end RF channelizer [3], an IF mixler [4], and other micromechanical circuits with so little loss that they eliminate the need for the RF LNA and transistor mixer of Fig. 1(a), thereby lowering power consumption and enhancing linearity (i.e., robustness).

In the circuit of Fig. 1(b), the RF channel-select filter bank is perhaps the key to greater performance, since it alone allows substantial simplification of circuits further
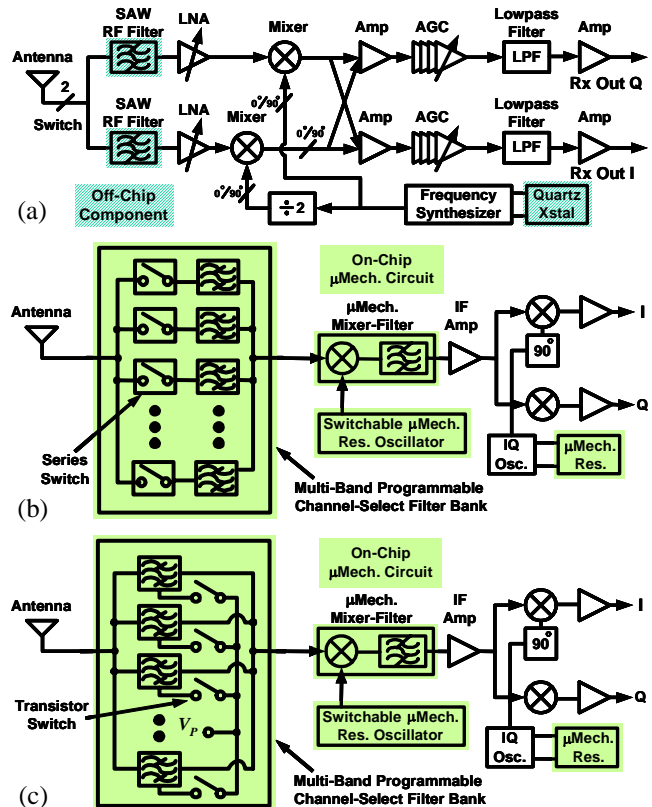

Fig. 1: Expected progression of transceiver front-end architectures when vibrating RF MEMS are employed. (a) Direct-conversion architecture. (b) Highly reconfigurable, low-power, RF channel-select architecture with series switches in its filter bank. (c) Improvement over Fig. 1(b) via use of self-switching RF filters in the channel selector, instead of lossy series switches.

down the receive path. In particular, an RF channel-select filter bank such as in Fig. 1(b) [3] would be capable of eliminating not only out-of-band interferers, but also out-of-channel interferers, relaxing the dynamic range requirements of the succeeding electronics to the point of perhaps allowing complete transceiver implementations using very low cost transistor circuits (e.g., organic transistors), or even purely mechanical ones. In Fig. 1(b), the RF channel-select filter bank is implemented using a multitude of micromechanical filters, each paired with a low loss switch in series. Among available switches, MESFET and

PIN diode switches are not competitive, since they consume considerable power and would contribute too much insertion loss when in series with the filters—insertion loss that adds directly to the noise figure of the overall receiver. RF MEMS switches, with insertion losses on the order of 0.1-0.2 dB and requiring very little switching power, should fare much better in this respect. However, they introduce other problems that might hinder their deployment, including excessive actuation voltages (20-80V for reliable operation), slow switching speeds (typically around 2-40 μs), and a perception of reliability issues (for some switch designs). Given all of the above impediments against attaining low loss switches on-chip, a method for switching a filter in and out without the need for series switches would be desirable.

Pursuant to attaining such a "self-switching" filter device, this paper describes bridged MEMS-based micromechanical filters that use a self-switching property of their dc-biased capacitive transducers to achieve zero-loss on/off filter switching without the need for lossy series switches, and with settling times down to 1.5 μs. By dispensing with the need for series switches in the signal path, a small bank of 0.087% bandwidth, 9-MHz beam-based filters has achieved programmable channel/band selection with only 3 dB of insertion loss, comprised entirely of filter loss (i.e., no switch loss), with switching times 7x faster than the typical 10 μs of some of the fastest RF MEMS switches, and without the high actuation voltages (>90V) and reliability issues often associated with RF MEMS switches. In addition, higher frequency disk resonators at 155 MHz achieve even faster switching speeds, with settling times down to only 430 ns. Equipped with this self-switching property, capacitively transduced micromechanical resonators now surface as attractive candidates for realization of switchable filter banks targeted for future wireless transceivers. If implemented with capacitively transduced filters using the self-switching concept described herein, the topology of Fig. 1(b) reduces to that shown in Fig. 1(c).

II. SELF-SWITCHING CAPACITIVE TRANSDUCER

The self-switching property harnessed in this work arises by virtue of its use of capacitive transducers to drive and sense vibrational resonances. In particular, because their electromechanical coupling efficiencies are strong functions of the bias voltage applied across their capacitive gaps [5], capacitive transducers are highly reconfigurable, much more so than other transducer approaches (e.g., piezoelectric, magnetomotive, etc.). For example, simply switching a bias voltage from 0V to 5V switches a capacitively transduced micromechanical resonator device from "off" to "on". Subsequent addition of a local oscillator signal to the bias voltage converts the device into a mixer-filter, or mixler [4].

Pursuant to obtaining a quantitative model describing the switching behavior of a micromechanical resonator device, Fig. 2(a) presents the cross-section of a capacitively transduced, two-port clamped-clamped beam micromechanical resonator in a typical two-port bias and excitation configu-
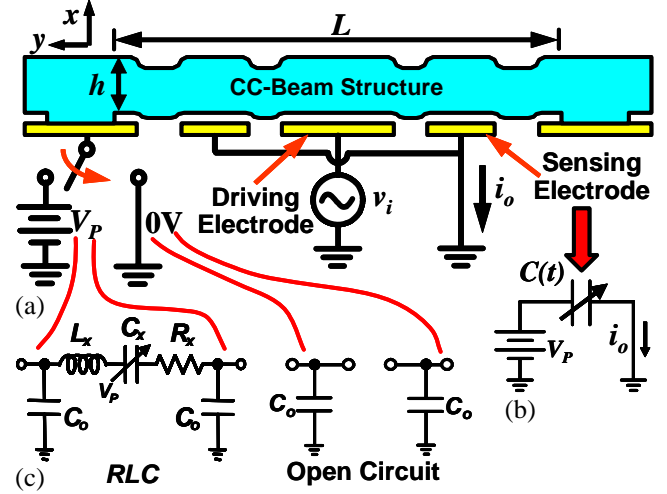

Fig. 2: (a) Cross-section of a clamped-clamped beam resonator under a two-port bias and excitation scheme. (b) Equivalent circuit modeling the output current generated by the dc-biased time-varying capacitance present during beam vibration. (c) Equivalent models for the device of (a) in its two states: *RLC* circuit when the device is "on"; and open circuit when the device is "off".

ration. As shown this resonator consists of a conductive beam fixed at both ends with an electrode positioned underneath that can electrostatically drive the beam into vertical resonance. To generate an electrostatic force at the frequency of the input excitation, a dc-bias voltage V_P is added to the input ac voltage v_i in order to remove a voltage-to-force rectification that would otherwise ensue. This dc-bias is normally applied separately from the ac input, to a separate lead connected directly to the resonant beam structure. (Note that no current flows once the structure is charged to V_P, so there is no dc power consumption.) With this combination of voltages, the force driving the beam into resonance vibration can be written

$$F_d = \frac{1}{2}\left(\frac{\partial C}{\partial x}\right)(V_P - v_i)^2 \cong -V_P\left(\frac{\partial C}{\partial x}\right)v_i \qquad (1)$$

where $\partial C/\partial x$ is the change in electrode-to-resonator overlap capacitance per unit displacement of the resonator; and where the expression on the far right retains only terms that act at the frequency of v_i. Once the frequency of v_i matches the beam resonance frequency, given by

$$f_0 = 1.03\sqrt{\frac{E}{\rho}}\frac{h}{L^2} \qquad (2)$$

where E and ρ are the Young's modulus and density of the structural material, respectively; and h and L are specified in Fig. 2(a); the beam begins to vibrate with significant amplitude, effectively generating the time-varying electrode-to-resonator capacitor circuit of Fig. 2(b) at its output port, for which the output motional current i_o is given by

$$i_o = V_P\left(\frac{\partial C}{\partial t}\right) = V_P\left(\frac{\partial C}{\partial x}\frac{\partial x}{\partial t}\right) \qquad (3)$$

where x is vertical displacement.

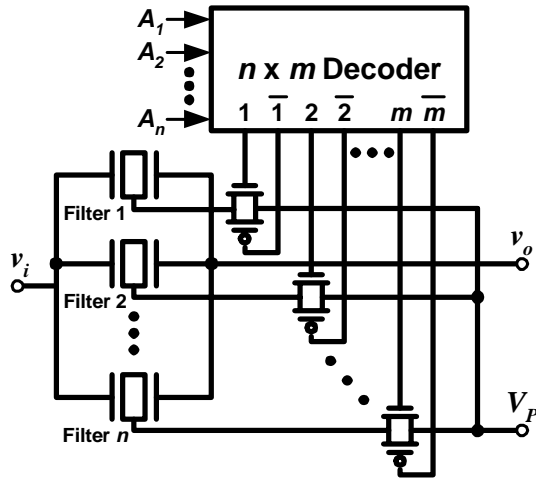From (1), the drive force goes to zero when $V_P = 0$V, in-

Fig. 3: System/circuit block diagram for an RF channel-select micromechanical filter bank that does not require low loss switches, but can rather just use CMOS pass gates for on/off switching by virtue of the self-switching provided by capacitive transducers.
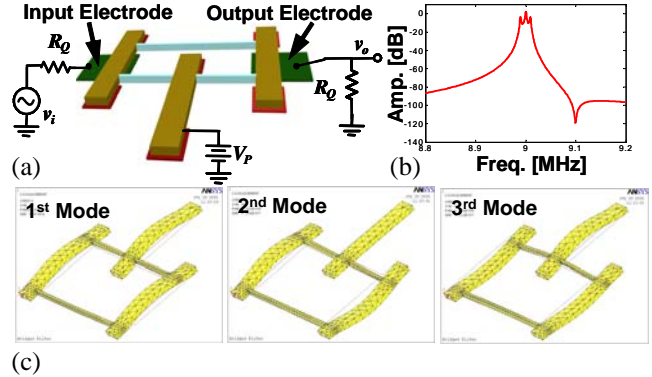

Fig. 4: (a) Perspective-view schematic of a bridged micromechanical beam filter, along with the preferred bias, excitation, and sensing circuitry. (b) Expected force-to-displacement mechanical frequency characteristic. (c) Finite element simulated mode shapes for this filter.

dicating that the resonator device can be electrically shut off by merely switching its dc-bias from a finite value (e.g., 5V) to zero. Furthermore, from (3), switching V_P to 0V also zeroes the output current, meaning that even if the beam were driven into motion by other forces (e.g., aliased forces from other input frequencies, microphonics, etc.), it still would produce no output current. In effect, the device is on/off self-switchable via the charge applied to its resonant structure: when the charge is such that $V_P = 0$V, the device is off; when the charge is such that V_P = finite, the device is on, and its impedance can be tailored by choice of V_P.

An important feature and advantage of the described self-switching capability is that because the switching mechanism is not directly in the signal path, it adds no insertion loss to this path. In other words, only the switched resonator or filter itself contributes insertion loss, not the charging mechanism. This means the charging switch need not be a low loss device, but can rather just be a transistor switch, or pass gate, perhaps controlled by a digital decoder circuit. The implementation of a switched filter bank might end up being as simple as that shown in Fig. 3, where all switching is done via CMOS pass gates to the dc-bias ports of each filter in the bank, with no need for low loss RF MEMS switches.

Fig. 2(c) presents equivalent circuits for the device of Fig. 2(a) for the two cases: (1) where a finite V_P is applied, in which case the device functions as an *LCR* terminated by shunt electrode-to-resonator overlap capacitors C_o; and (2) where $V_P = 0$V, in which case the device is an effective open circuit, but shunt electrode-to-resonator capacitors still load the input and output lines. This load capacitance might become an issue when implementing very large filter banks, so its value could be of importance in some cases. If so, then the shunt capacitance can be removed (with some added complexity) by open-circuiting the resonator or filter struc-

ture once discharged to 0V, and perhaps using non-conductive coupling beams in the filter structure (as in [4]) to suppress input-to-output feedthrough.

Of course, among the parameters gauging switch performance, switching time is one of the most important. As will be detailed more explicitly in Section IV, the time required to dc-bias switch a micromechanical resonator on or off is a function of two competing phenomena: (1) the time required to charge the resonant structure, governed mainly by the capacitances involved; and (2) the time required for mechanical transients induced by the voltage switch to settle. As will be seen in Section IV, the latter dominates the total switching time in most cases.

III. SELF-SWITCHING MICROMECHANICAL FILTER

Fig. 4(a) presents the perspective-view schematic for a capacitively transduced bridged micromechanical filter comprised of three clamped-clamped beam resonators coupled by soft flexural mode mechanical coupling beams [6]. This filter design utilizes coupling of non-adjacent resonators (i.e., "bridging") to achieve a low insertion loss frequency shaping transfer function with sharper passband-to-stopband roll-offs than achievable by non-bridged counterparts. As detailed more fully in [6], the center frequency of this filter is determined primarily by the (identical) frequencies of its constituent resonators, while the spacings between modes (i.e., the bandwidth) is determined largely by the stiffnesses of its coupling beams. Fig. 4(c) presents
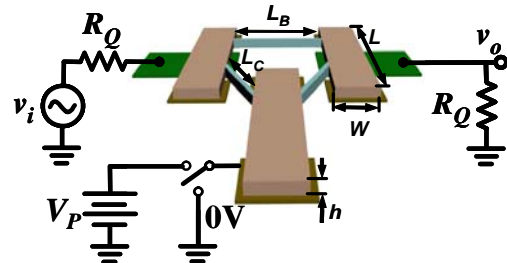

Fig. 5: Perspective-view schematic of a bridged micromechanical beam filter with a switch to allow filter operation when the device is "on", and open circuit when the device is "off".
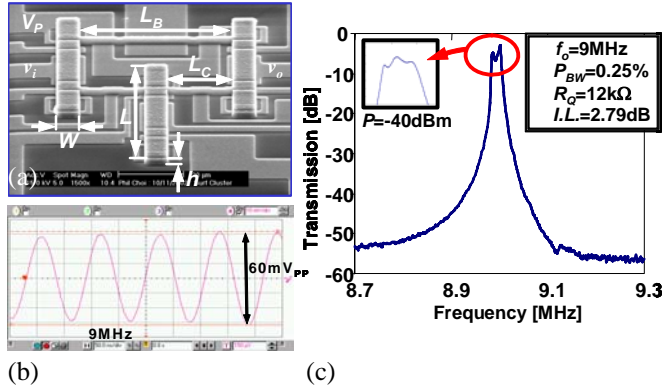
Fig. 6: (a) SEM, (b) time-domain response, and (c) measured frequency characteristic for a fabricated 9-MHz bridged micromechanical filter.

finite element simulations depicting the mode shapes corresponding to each of the three mode frequencies in the filter force-to-displacement frequency characteristic of Fig. 4(b).

Since capacitively transduced filters operate virtually identically to two-port resonators, with an input signal applied to the input electrode, a dc-bias applied to the (more complex) resonant structure, and the output taken at the output port, the procedure for self-switching is also identical, and is summarized in Fig. 5. The equivalent model is further similar to that of Fig. 2(c), except with the *LCR* replaced with the full micromechanical filter equivalent circuit [6].

IV. EXPERIMENTAL RESULTS

Fig. 6(a) presents the SEM of one of the fabricated bridged micromechanical beam filters used to evaluate self-switching in this work, along with a frequency characteristic measured under vacuum, as well as the oscilloscope waveform seen under an in-band sinusoidal input. As shown, this filter is centered at 9 MHz and achieves an insertion loss of only 2.79 dB for a 0.25% bandwidth, with an impressive 51 dB of stopband rejection. Table 1 summarizes the design dimensions and dc operating conditions used for this filter.

To best illustrate the utility of self-switching, a small two-resonator filter bank was hooked up as depicted in Fig. 7(a). Here, two filters, one at 9.41 MHz, the other at 9.57 MHz, are hooked in parallel, with a common input and a common output, and with separate switches to dc-bias voltages $V_{P1} = V_{P2} = 4$V. The operation of the filter bank was verified by first measuring its frequency response under

Table 1: Bridged Micromechanical Filter Summary

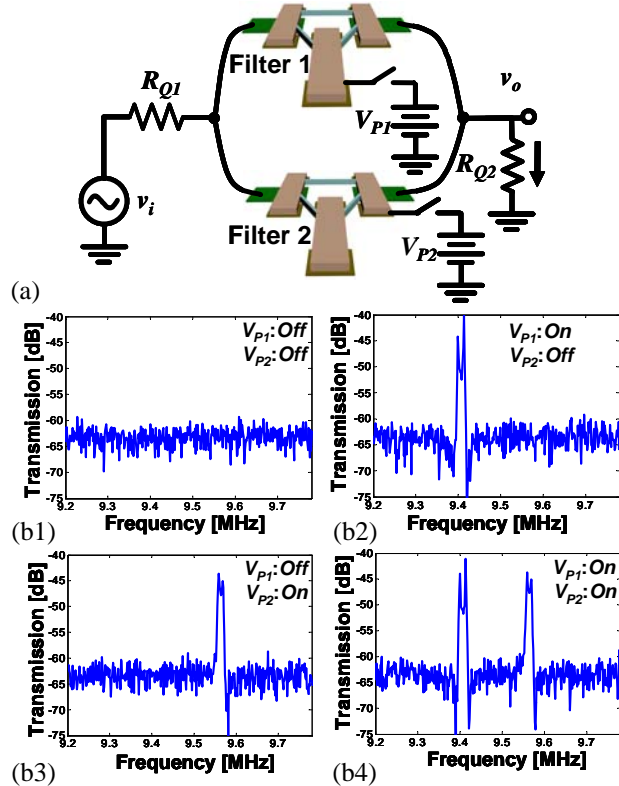| Design/Operation Parameters	Value	Unit
Beam Length, *L*	40	μm
Beam Width, *W*	6	μm
Beam Thickness, *h*	2	μm
Electrode-to-Resonator Gap, d_0	100	nm
Filter DC-Bias Voltage, V_P	10.47	V
Center Frequency, f_0	9	MHz
Percent Bandwidth, P_{BW}	0.25%	-

Fig. 7: (a) Perspective-view schematic of a two-filter self-switching micromechanical filter bank with switches to allow channel-selection via filter dc-bias ports. (b) Frequency characteristics chronicling the channel-selection effected by the self-switching micromechanical filter bank with (b1) both channels off, (b2) 1st channel on and 2nd channel off, (b3) 1st channel off and 2nd channel on, and (b4) both channels on.

all of its states as presented in Fig. 7(b) and summarized as follows:

1) Fig. 7(b1): With all dc-bias voltages off (i.e., 0V), there is no frequency response, verifying a fully off state;

2) Fig. 7(b2): With $V_{P1} = 4$V (on) and $V_{P2} = 0$V (off), filter 2 is off, while filter 1 operates normally and the 1st channel appears in the frequency response spectrum;

3) Fig. 7(b3): With $V_{P1} = 0$V (off) and $V_{P2} = 4$V (on), filter 1 is off, while filter 2 operates normally and the 2nd channel appears in the frequency response spectrum; and

4) Fig. 7(b4): When both dc-bias voltages are on, both channels appear in the frequency response spectrum, allowing dual tones to pass simultaneously.

Although the above experiments only demonstrate a small filter bank at a relatively low frequency of 9 MHz, it is reasonable to expect a straightforward extension of the quantity to hundreds or thousands of filters in a bank using geometries capable of the much higher RF frequencies needed by present and future wireless communication standards.

Next, the switching speed of the filter of Fig. 7(a) was measured by observing its output transient response when a step dc-bias voltage is applied directly to its resonant structure with different input powers applied at 9 MHz to its in-
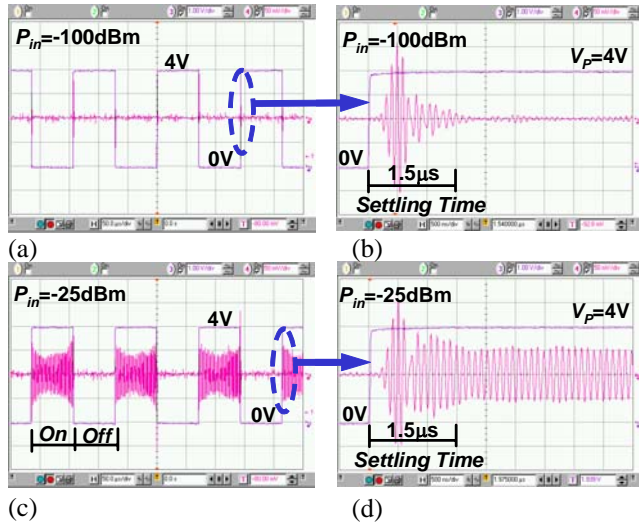
Fig. 8: Time domain response waveforms for a self-switching micromechanical filter. (a) Without RF input (-100 dBm). (b) Time scale zoom-in on (a). (c) With RF input (-25 dBm). (d) Time scale zoom-in on (c).

put. Fig. 8(a) presents the measured oscilloscope waveform capturing the transient output response of the filter (under 20 µTorr vacuum) with practically no input (i.e., input power = -100 dBm) with a square-wave applied to its switch port (i.e., its dc-bias port). Fig. 8(b) presents the same plot with a zoomed time scale, revealing an under-damped settling response following each 4V "switch on" step, apparently governed by the under-damped mechanical response of the filter structure. The settling time to steady-state was measured to be about 1.5 µs, which is better than that of the majority of existing micromechanical switches. The frequency of the under-damped response at 9 MHz corresponds to the frequency of first mode of the filter structure, and this is verified by further mechanical analysis (beyond the scope of the present paper).

Fig. 8(c) presents the measured oscilloscope waveform capturing the output transient response of the filter (under 20 µTorr vacuum), again, with a square wave applied to its switch port, but this time with a -25 dBm input signal applied to its input port. As expected, the input signal is passed only during the 4V "on" cycles of the applied square wave, verifying once again the self-switching function of the filter. Fig. 8(d) presents the same plot with a zoomed time scale

Table 2: Performance Comparison of Switches and Self-Switching Micromechanical Circuits

	MESFET	PIN Diode	MEMS	Self-Switching
Series Resist. (mΩ)	3-5	1	< 1	~0
Loss at 1GHz (dB)	0.5-1.0	0.5-1.0	0.1	~0
Isolation (dB)	20-40	40	> 40	> 50 (filter)
IIP3 (dBm)	40-60	30-45	> 66	filter IIP3
1dB Comp. (dBm)	20-35	25-30	> 33	filter 1dB Comp.
Size (mm²)	1-5	0.1	< 0.1	~0
Switching Speed	~ ns	~ µs	> 5µs	< 2µs
Control Volt. (V)	8	3-5	3-30	filter V_P
Control Current	<10µA	10mA	< 10µA	~0

similar to that of Fig. 8(b), showing an output time-domain response with a settling behavior obtainable via the superposition of the dynamic responses of (1) a filter structure under the step force applied to its switch port; and (2) an in-band signal passing through the filter (which grows exponentially with a time constant proportional to the inverse of the filter bandwidth). From the figure, the initial response is obviously dominated by the step force generated at its switch port, while the response in steady-state is governed by that of its in-band RF input signal. The settling time (i.e., switching speed) is again an impressive 1.5 µs.

Armed with the above measured results, Table 2 compares the switching characteristics of the present self-switching micromechanical filter with those of other popular switches, including conventional MESFET switches, PIN diode switches, and RF MEMS switches [7]. As shown, because the mechanism of self-switching for the filter effectively does not introduce any switching loss in the signal path (i.e., all the loss is due to the filter, not the switch mechanism), its effective insertion loss of 0 dB is superior to that of any of the other switches. In addition, its energy requirement per switch is comparable to that of RF MEMS switches, while its speed and reliability are better, the latter of these coming about because no actual contact is made when switching occurs. All tolled, the present self-switching filter device appears to be on par or superior in every tabulated category.

V. SELF-SWITCHING MICROMECHANICAL DISK FILTER

To investigate the self-switching performance of filters with higher frequency than attainable by beam-based designs, ones based on radial contour-mode disk geometries were also explored. In particular, Fig. 9(a) presents the SEM of a 155-MHz two-resonator contour-mode disk filter, fabricated via a three polysilicon self-aligned-and-filled stem process previously used to attain GHz resonators [8]. The design and performance of this filter is described more fully in [9], but like its beam-based counterpart, its center frequency is determined mainly by the radius of its constituent (and identical) disks, while its bandwidth is set by the dimensions of its coupling beams and their specific attachment locations [9]. In essence, the passband of this disk filter is defined by its in-phase and out-of-phase modes, illustrated by the ANSYS simulations of Fig. 9(b). Fig. 9(c) presents the unterminated frequency response of this filter, where the two vibrating mode peaks centered around a 155 MHz center frequency are clearly seen.

Fig. 10(a) presents the measured switched dynamic response of a disk filter with no power applied to its input, but with a square wave voltage applied to its switch port (i.e., to the disk structure), again showing an under-damped mechanical response with a settling time now down to 430 ns—much faster than the previous beam-based filter structure. Fig. 10(b)-(d) present measured dynamic response waveforms with input power applied, showing rejection of this power at the output (but with some feedthrough at this

(a) (b)

R=17μm
h_r=3μm
$d_{Nitride}$=200Å
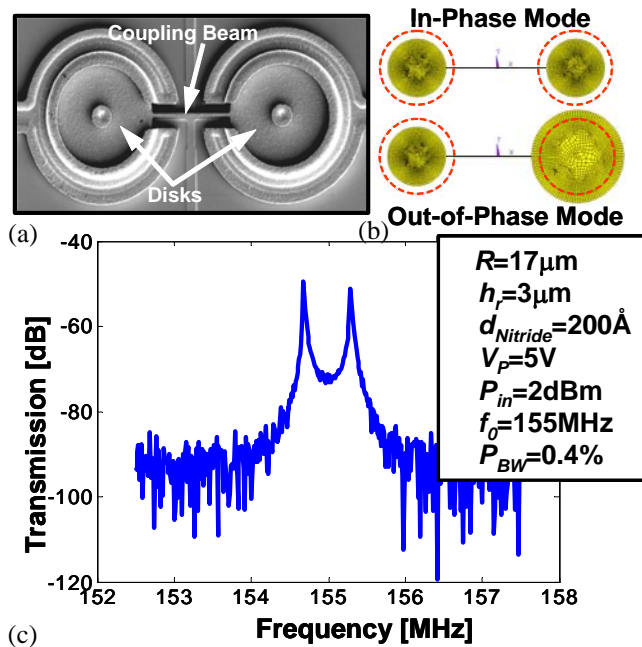V_P=5V
P_{in}=2dBm
f_0=155MHz
P_{BW}=0.4%

(c)

Fig. 9: (a) SEM (b) ANSYS-simulated mode shapes, and (c) measured spectrum for a fabricated 155-MHz two-resonator micromechanical contour-mode disk filter.

(a) f_0=34MHz   (b) f_0=155MHz

Fig. 11: (a) Switched dynamic mode and (b) filter mode for each constituent resonator of the disk filter in Fig. 9(a).

tually provides advantages on two fronts for filters based on laterally vibrating resonators, since (1) the flexural out-of-plane mode of the step force response dampens much more quickly (due to viscous gas damping [10]) than the in-plane filter modes, allowing a much faster settling time; and (2) there is an opportunity to completely dampen out the step force response without affecting the overall filter response. Investigations into the latter are presently underway.

VI. CONCLUSIONS

MEMS-based micromechanical filters have been demonstrated that use a self-switching property of their dc-biased capacitive transducers to achieve zero-loss on/off filter switching without the need for lossy series switches, and with settling times down to 430 ns. By dispensing with the need for series switches in the signal path, programmable channel/band selection has been demonstrated, with no switch loss (i.e., only filter loss), no extra die area consumption, and with switching times much faster than that of RF MEMS switches. Equipped with this self-switching property, capacitively transduced micromechanical resonators may soon become leading candidates for realization of the large switchable filter banks targeted for future wireless transceivers.

In particular, it is the self-switching property of its capacitive transducers that allows the multi-band programmable channel-select filter bank of Fig. 1(c) to be realized via the very simple transistor-switch system block depicted in Fig. 3 [11]. As shown, this block consists of a bank of micromechanical filters with filter inputs connected to a common block input and all outputs to a common block output, and where each filter passband corresponds to a single channel in the communication standard of interest. In the scheme of Fig. 3, a given filter is switched on (with all others off) by decoder-controlled application of an appropriate dc-bias voltage to the desired filter. If the potential of micromechanical circuit technology is as big as predicted, the circuit of Fig. 3 is merely an inkling of what might be possible with the mechanical integration density to be enabled via MEMS technology.

much higher frequency) with V_P = 0V, and passing of signal power with V_P = 4V. The time-scale zoom-in of Fig. 10(d) again shows an impressive 430 ns settling time.

Interestingly, the frequency of the settling oscillations in Fig. 10(a) is not the 154.7 MHz filter first mode frequency, but rather only 34 MHz. This is because unlike the previous beam-based filter of Fig. 4, the switched dynamic mode of the disk filter structure is dictated by its fundamental out-of-plane vibrating mode, shown in the ANSYS simulation of Fig. 11(a), which is different from any of its in-plane filter modes, as shown in Fig. 11(b). Again, this differs substantially from the vertically-resonant beam filter of Fig. 4, for which the settling time was determined mainly by the response of the first filter mode. The fact that the step force response mode is different from any of the filter modes ac-
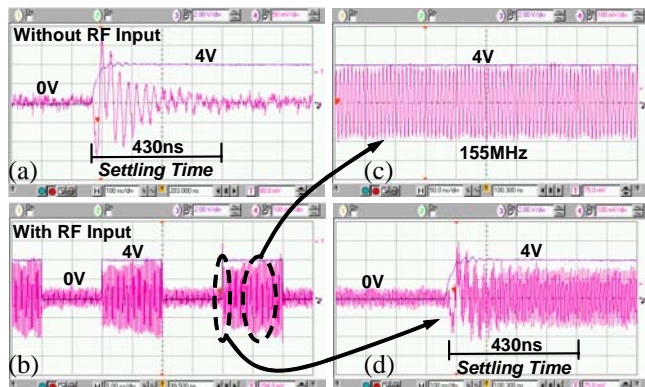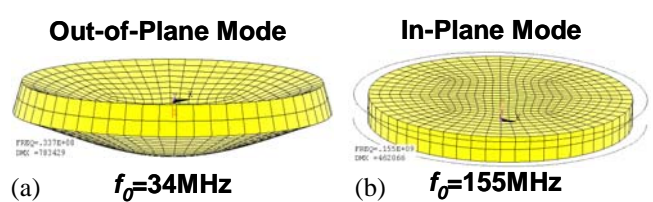

Fig. 10: Time domain responses of a self-switching micromechanical disk filter. (a) Without RF input (-100 dBm). (b) With RF input (-25 dBm). (c) zoom-in on the steady-state portion of (b). (d) zoom-in on the transient response of (b).

References.
[1] P. Zhang, *et al.*, "A CMOS direct-conversion transceiver for IEEE 802.11a/b/g WLANs," *Proceedings,* 2004 IEEE Custom Integrated Circuits Conf., Orlando, Florida, Oct. 3-6, 2004, pp. 409-412.

S.-S. Li, Y.-W. Lin, Z. Ren, and C. T.-C. Nguyen, "Self-switching vibrating micromechanical filter bank," *Proceedings*, Joint IEEE Int. Frequency Control/Precision Time & Time Interval Symposium, Vancouver, Canada, Aug. 29-31, 2005, pp. 135-141.

[2] Analog Devices AD6548 Othello-G Data Sheet.

[3] C. T.-C. Nguyen, "Vibrating RF MEMS for next generation wireless applications," *Proceedings*, 2004 IEEE Custom Integrated Circuits Conf., Orlando, Florida, Oct. 3-6, 2004, pp. 257-264.

[4] A.-C. Wong and C. T.-C. Nguyen, "Micromechanical mixer-filters ("Mixlers")," *IEEE/ASME J. Microelectromech. Syst.*, vol. 13, no. 1, pp. 100-112, Feb. 2004.

[5] H. Nathanson, W. E. Newell, R. A. Wickstrom, and J. R. Davis, Jr., "The resonant gate transistor," *IEEE Trans. Electron Devices*, vol. ED-14, pp. 117-133, Mar. 1967.

[6] S.-S. Li, M. U. Demirci, Y.-W. Lin, Z. Ren, and C. T.-C. Nguyen, "Bridged micromechanical filters," *Proceedings*, IEEE Int. Ultrasonics, Ferroelectrics, and Frequency Control 50th Anniv. Joint Conf., Montreal, Canada, Aug. 24-27, 2004, pp. 144-150.

[7] G. M. Rebeiz and J. B. Muldavin, "RF MEMS switches and switch circuits," *IEEE Microwave Magazine*, Dec. 2001, pp. 59-71.

[8] J. Wang, Z. Ren, and C. T.-C. Nguyen, "1.156-GHz self-aligned vibrating micromechanical disk resonators," *IEEE Trans. Ultrason., Ferroelect., Freq. Contr.*, vol. 51, pp. 1607-1628, Dec. 2004.

[9] S.-S. Li, Y.-W. Lin, Z. Ren, and C. T.-C. Nguyen, "Disk-array design for suppression of unwanted modes in micromechanical composite-array filters," *Technical Digest*, 2006 IEEE Int. Conf. on Micro Electro Mechanical Systems, Istanbul, Turkey, Jan. 22-26, 2006, to be published.

[10] Y.-H. Cho, A. P. Pisano, and R. T. Howe, "Viscous damping model for laterally oscillating microstructures," *J. Microelectromech. Syst.*, vol. 3, no. 2, pp. 81-87, June 1994.

[11] C. T.-C. Nguyen, "Micromechanical circuits for communication transceivers (invited)," *Proceedings*, 2000 Bipolar/BiCMOS Circuits and Technology Meeting (BCTM), Minneapolis, Minnesota, September 25-26, 2000, pp. 142-149.